Published in final edited form as:
J Control Release. 2011 February 28; 150(1): 77–86. doi:10.1016/j.jconrel.2010.10.002.

Oral TNF-α Gene Silencing using a Polymeric Microsphere-Based Delivery System for the Treatment of Inflammatory Bowel Disease

Christina Kriegel and **Mansoor Amiji**
Department of Pharmaceutical Sciences, School of Pharmacy, Northeastern University, 110 Mugar Life Sciences Building, Boston MA 02115 (Tel. 617-373-3137)

Mansoor Amiji: m.amiji@neu.edu

Abstract

The purpose of this study was to evaluate down-regulation of tumor necrosis factor (TNF)-α by oral RNA interference therapy. Control (scrambled sequence) or TNF-α specific small interfering RNA (siRNA) was encapsulated in type B gelatin nanoparticles and further entrapped in poly(epsilon-caprolactone) (PCL) microspheres to form a **n**anoparticles-**i**n-**m**icrosphere **o**ral **s**ystem (NiMOS). Upon confirmation of the dextran sulfate sodium (DSS)-induced acute colitis model, mice were divided into several treatment groups receiving no treatment, blank NiMOS, NiMOS with scramble siRNA, or NiMOS with TNF-α silencing siRNA by oral administration. Successful gene silencing led to decreased colonic levels of TNF-α, suppressed expression of other pro-inflammatory cytokines (e.g., interleukin (IL)-1β, interferon (IFN)-γ) and chemokines (MCP-1), an increase in body weight, and reduced tissue myeloperoxidase activity. Results of this study established the clinical potential of a NiMOS-based oral TNF-α gene silencing system for the treatment of inflammatory bowel disease as demonstrated in an acute colitis model.

Keywords

Inflammatory bowel diseases; TNF-α; RNA interference; siRNA; oral delivery; nanoparticles-in-microsphere oral system (NiMOS)

Introduction

Inflammatory bowel disease (IBD), represented by two main phenotypes - Crohn's disease (CD) and ulcerative colitis (UC) - is a chronic relapsing condition involving inflammation of the gastrointestinal (GI) tract. While its aetiology is still unknown, a complex interaction of genetic disposition, environmental conditions, life style, microbial and immune factors have been identified as some of the major aspects leading to IBD (1,2). Conventional treatment consists of anti-inflammatory and immune-suppressive drugs (3), depending on the patient's clinical state including extent and severity of the disease. Some medications are effective measures to combat inflammation in the acute setting, but ineffective in maintaining remission due to toxicity, dependency and higher relapse rates (4). Another treatment option

Correspondence to: Mansoor Amiji, m.amiji@neu.edu.

is surgical removal of the inflamed intestinal tissue; however patients have to undergo a great deal of mental stress and physical suffering. Due to the limitations in efficacy and safety associated with the current treatment options, development of novel biological therapies involving selective blockage of mucosal inflammatory pathways, offer potential for more effective treatment options in IBD.

CD is usually associated with an exaggerated T-helper cell type -1 (Th1) reaction coupled with excess production of IL-12, IL-17, IFN-γ followed by upregulation of TNF-α and IL-1β, while UC is linked to a Th2 response, associated with secretion of IL-5 and IL-13 (2,5,6). It is widely accepted that TNF-α plays a central role in the mediation of inflammation in IBD (7). Thus, most biological therapy strategies are aimed at neutralization and reduction of this cytokine using specific monoclonal antibodies or soluble receptors via systemic administration (2,4,5,8–10). While such systemic anti-TNF-α therapy works well in patients refractory to conventional therapy, serious contraindications and side effects including opportunistic infections, antibody formation against anti-TNF-α in conjunction with decreased efficacy of the therapy, and increased occurrence of infusion reactions have been reported (5,9,10). Other treatment options for IBD include targeting of anti-IL-12 antibodies (11), anti-IL-6 receptor monoclonal antibodies (12) and anti-CD-3 antibody (13), $\alpha_4\beta_7$ integrins (14) for management of Crohn's disease and ulcerative colitis, respectively. Additionally, the concept of gene therapy for treatment of IBD has received significant attention, while the GI tract offers an ideal target due to the large surface area and access to the luminal site of inflammation via oral and rectal routes of administration allowing for local delivery of the treatment.

RNA interference therapy utilizes short interfering RNA (siRNA), usually composed of 20–25 nucleotides, and is involved in a gene-silencing mechanism through RNA interference where siRNA can ultimately block the expression of a specific gene, *e.g.* those expressed in diseases (15). Thus, application of siRNA can offer a alternative therapeutic strategy to overcome a disease. Our central hypothesis is that upon administration of siRNA encoding for one or more of the pro-inflammatory cytokines involved in the disease, their balance can temporarily be restored offering potential treatment of IBD. For example, it has been shown that pharmacological reduction of TNF-α decreased the severity of the disease in animal models and humans (16). While many siRNA studies are focused on cancer therapies (17,18), some include treatment of inflammatory disease (15,19–21). Currently, the biggest hurdle in gene silencing remains delivery and stability due to rapid degradation of siRNA in the cytoplasm and plasma (22). For this purpose, encapsulation and delivery mechanisms have been employed involving various systems including viral vectors (23), nanoparticles (20), polymer-based vehicles (21,24) or liposomal vesicles (15). Some success has been reported in systemic administration (15,18–20), although only very few studies discuss oral delivery of siRNA particles (21). Additionally, several companies, such as Novartis and Cequent, have programs in oral siRNA delivery for different types of diseases.

Among the challenges of oral siRNA delivery is to ensure a minimal degradation of the payload by gastric and intestinal enzymes, with maximized residence time of particles in the intestine. This allows for sufficient interaction with target cells, aiding in cellular uptake and endosomal release for efficient silencing in the cytosol. To this purpose, we have previously developed multicompartmental NiMOS carrying the hydrophilic labile payload in the innermost nanoparticulate phase of gelatin, released over time by a controlled degradation of the outer layer (25–27). This platform has been shown to efficiently encapsulate plasmid DNA, enable intracellular uptake, and nuclear transport while being safe and efficient for gene transfection (26,27). Moreover, we have shown that the microspheres with sizes smaller than 5μm will promote localization in the intestine by delivery of gelatin nanoparticles to the enterocytes, epithelial and other cells at these sites once the PCL matrix

is degraded by lipases abundantly present in the intestinal tract allowing for endocytosis (28). As such, it can be described as an effective system for siRNA encapsulation and delivery. In this preliminary study, we have encapsulated inactive (scrambled) or TNF-α specific siRNA in gelatin nanoparticles forming NiMOS to evaluate the potential of oral delivery by showing evidence or oral TNF-α gene silencing in IBD by administration in a DSS-induced acute colitis mouse model.

Materials and Methods

Formulation of gelatin nanoparticles and NiMOS encapsulating siRNA

Gelatin nanoparticles (Type B, 225 bloom strength, MW 40,000–50,000, 100–115 mM of free carboxylic acid per 100g of protein, pI of 4.7–5.2) were exactly prepared as described before (25,29,30). In brief, siRNAs were mixed with aqueous gelatin solutions (pH 7.0) and pre-incubated for 10 min at room temperature followed by controlled precipitation of siRNA-containing or blank gelatin solutions with the aid of ethanol as the non solvent. Desalted and annealed siRNAs were obtained from Dharmacon (Lafayette, CO); their sequences are shown in supplementary Table S1. In the final blend, the ethanol-to-water volume ratio was kept constant at 65:35. The resulting nanoparticles were centrifuged at 32,000rpm for 45 min, purified and lyophilized. The nanoparticle-in-microspheres-oral delivery system (NiMOS) was manufactured by utilizing the “double emulsion-like” technique, which has been employed previously by numerous other researchers (25,30) and is frequently used for production of microparticulate delivery systems in the pharmaceutical industry (31,32).

Characterization of gelatin nanoparticles and NiMOS encapsulating siRNA

Particle size analysis—Freshly prepared nanoparticle formulations were characterized for the mean particle size of the droplets using the Malvern Zetasizer Nano ZS 90 apparatus (Westborough, MA) at a 90° scattering angle. NiMOS were characterized for particle size and size distribution using Multisizer™ 3 from Beckman Coulter (Fullerton, CA). All sizing measurements were carried out at room temperature.

Scanning electron microscopy (SEM)—Lyophilized blank or loaded gelatin nanoparticles and NiMOS samples were sputter coated with gold-palladium to minimize surface charging and evaluated according their surface morphology with a Hitachi S4800 (Pleasanton, CA) field emission scanning electron microscope.

Determination of siRNA loading in gelatin nanoparticles and NiMOS—siRNA-loaded gelatin nanoparticles and NiMOS were prepared as discussed above. Encapsulation efficiency of siRNA in these formulations was determined by dissolving a known amount of sample (~50mg) in phosphate buffered saline (PBS, pH 7.4) containing 0.2mg/ml protease (Sigma, St. Louis, MO)at 37°C until a clear solution was obtained. Released siRNA was quantified using the PicoGreen® assay (Invitrogen, Carlsbad, CA) according to the manufacturer’s protocol. The intensity of fluorescence which is proportional to the PicoGreen® bound siRNA was measured at an excitation of 485nm and emission of 520nm wavelengths using a Perkin Elmer LS50B spectrophotometer (Norwalk, CT). FLWINLAB® software was used for processing and analysis of resulting data.

Evaluation of siRNA loading in NiMOS was carried out as described before (28). Briefly, ~100mg of sample was added to 1ml of dichloromethane to dissolve the PCL matrix and liberate the gelatin nanoparticles. To this organic PCL-dicholoromethane mixture, an equal amount of distilled deionized water was added. After careful separation of the aqueous from the organic phase, gelatin nanoparticles underwent the same procedure as described above to

measure the final siRNA loading efficiency in the NiMOS using the PicoGreen® quantitation assay.

siRNA stability—To ensure that the manufacturing process of gelatin nanoparticles of NiMOS did not affect the integrity of siRNA, stability of encapsulated siRNA was assessed by agarose gel electrophoresis. Additionally, the integrity of the payload in the presence of RNAse A was determined. To this purpose, a sample of siRNA containing NiMOS was treated with RNAse A for 20min at 37°C followed by inactivation of the enzyme and extraction of siRNA from loaded nanoparticles by protease digestion of the gelatin matrix that were extracted in the same manner as discussed above. After siRNA release from microspheres and nanoparticles, samples were added to the wells of a 4% (w/v) pre-stained E-gel™ (Invitrogen) and run against a 10bp ladder, naked siRNA, naked siRNA treated with protease, and naked siRNA treated with protease and RNAse A as controls on an E-gel™ electrophoresis system. After a 40 min run at 70V, the image was recorded under UV light and processed with the Kodak imaging software.

In Vivo Evaluation and Gene Silencing and Efficacy

Experimental Animals—All animal studies involved were performed in accordance with the experimental protocol approved by the Institutional Animal Care and Use Committee at Northeastern University (Boston, MA). Female Balb/c mice (6–8 weeks, ~18–20g) were purchased from Charles River Laboratories (Wilmington, MA). Animals were randomly assigned to groups of 4 mice per cage and acclimatized for 10 days before the start of the study. The mice were housed in rooms at a controlled temperature of 22°C and 26% humidity, with light-dark cycles of 12 hours and fed with water and a standard pellet *at libitum* except when fasted overnight to prepare for the oral gavage.

Induction of acute colitis using dextran sodium sulfate (DSS)—Animals were randomly assigned to ten groups (n=4). Acute colitis was induced in mice by addition of 3.5% (w/w) DSS (MW 36,000 – 50,000) in their drinking water for the duration of the study, while one control group (n=8) received regular tap water throughout the course of the study. DSS solutions were freshly prepared on daily and mice were monitored every day for their health condition (33). The acute disease model was confirmed by evaluation of weight loss, stool consistency, rectal bleeding, and tissue histology. At day 10 and 14 of the study, animals were sacrificed by CO_2 inhalation followed by cervical dislocation and tissue was processed as described below.

Oral siRNA administration in DSS colitis-induced Balb/c mice—On day 2, 4, and 6 of the study, mice of all groups including controls were fasted overnight followed by administration of blank NiMOS (unloaded particles), scrambled or TNF-α siRNA loaded NiMOS (1.2mg/kg body weight in 200μl final volume) per animal by oral gavage using a blunt-tipped feeding needle inserted into the esophagus equivalent to three doses of NiMOS formulations per group. An additional control group consisted of animals receiving no oral treatment throughout the course of DSS exposure (DSS control). It is worth mentioning that this study represents a preliminary evaluation of the formulation rather than a full-fledged body of work. Additional studies are needed to examine chronic benefits as well as potential toxicity of the formulations.

At predetermined time points of 3 and 7 days post-administration (day 10 and 14, respectively), 4 animals per time point and group were sacrificed. After euthanasia, the large intestine was surgically removed and carefully washed with PBS for histological analysis of the tissue sections and determination of cytokine and murine TNFα –mRNA levels by Multiplex ELISA and real-time PCR, respectivley.

Isolation of RNA from colon tissue and quantitative polymerase chain reaction—Tissue samples obtained from the large intestine were stored in RNA*later*® (Applied Biosystems Inc., Foster City, CA) at 4°C for two days to allow enough time for tissue penetration followed by removal of excess liquid and storage of tissue at −70°C until processing. RNA was isolated from tissue samples using the guanidine isothiocyanate method supplied in the RNAqueous® - 4PCR kit (Applied Biosystems Inc., Foster City, CA) according to the manufacturer's protocol. The isolated RNA from the tissue samples was quantified using the NanoDrop 1000 (Thermo Fisher Scientific Inc., Wilmington, DE) UV-Vis spectrophotometer.

Synthesis of cDNA from isolated mRNA by reverse transcription—After determination of the RNA concentration, cDNA was synthetized from RNA using the Superscript III First-Strand Synthesis SuperMix for qt-PCR (Invitrogen, Carlsbad, CA). The preparation for reverse transcription of RNA samples was performed on ice and in accordance with the manufacturer's recommendation. A volume corresponding to 1 μg of RNA as determined by UV spectrophotometric analysis was used for the synthesis process. Samples containing cDNA were diluted to a final volume of 100μl and used for subsequent quantitative real time PCR.

Quantitative analysis of cDNA by quantitative polymerase chain reaction—Quantitative real time polymerase chain reaction (qPCR) was performed on cDNA samples obtained from large intestinal tissue to determine the levels of mRNA transcript. L32 gene expressing the L32 ribosomal protein served as a control. Pre-diluted cDNA was mixed with 0.2 μM of primer pair detecting the murine TNF-α or L32 construct and SYBR® Green pcr master mix and pipetted into an ABI Prism™ 96-well optical reaction plate (Applied Biosystems, Foster City, CA). The sequences of the primers used are shown in supplementary Table S1. The quantitative PCR reaction was performed in the 7300 Real-Time PCR System from Applied Biosystems using the following cycle program: 40 cycles 95°C for 15 seconds; 60°C for 1 minute. Results obtained from the PCR reaction were analyzed by comparative Ct analysis to determine the relative amount of murine TNF-α cDNA in the samples.

Determination of tissue murine cytokine expression levels by ELISA—For subsequent ELISA and measurement of myeloperoxidase activity, samples of the entire large intestine were homogenized in lysis buffer (1M TRIS, pH 7.4; 0.5M EDTA, pH 8.0; 5M NaCl, 10% (w/v) Brij, 10% (v/v) Tween 20), supplemented with proteinase inhibitor, on ice to extract the proteins from the tissue samples. Protein containing supernatant was separated by centrifugation at 13000g for 30min at 4°C and stored at −70°C until analysis. The Q-Plex™ Mouse Cytokine Screen ELISA obtained from Quansys Biosciences (Logan, UT) was used to measure changes in concentration of a series of pro- and anti-inflammatory cytokine (TNF-α, IL-1α, IL-1β, IL-2, IFN-γ, IL-5, IL-6, IL-12p70, IL-17, MIP-1α, MCP-1, and GMCSF) in the large intestine of colitis-induced Balb/c mice according to the manufacturer's protocol. Luminescence intensity of each sample was measured and the concentration of each cytokine was analyzed with a five-parameter curve fitting using the Q-View™ software (Quansys Biosciences). Cytokine concentrations obtained from the multiplex ELISA were normalized against the total protein content of each individual sample as determined by bicinchoninic acid assay (Pierce, Rockford, IL). Values are expressed as pictogram (pg) or femtogram (fg) of murine cytokine expressed per mg of total protein content of each sample and represent mean ± S.D. of four mice.

Histological analysis of tissue sections by H&E staining—Tissue samples were evaluated for mucosal architectural change, cellular infiltration, inflammation, goblet cell

depletion, surface epithelial cell hyperplasia, and signs of epithelial regeneration by using light microscopy of hematoxylin and eosin survey staining (33,34). These values were used to assess the degree of mucosal damage and repair in treatment and control groups. Tissue samples harvested from distal regions of the non-/inflamed colon were stored in 10% formalin solution at 4°C for at 7 days to fix the tissue. After that, samples were washed with PBS to remove excessive formalin solution and then transferred to 30% (w/w) sucrose solution for 2 days to prepare for subsequent cryosectioning of the tissue with the purpose of protection from freezing damage. Tissue sections with a thickness of 7 μm were stained with haematoxylin and eosin according to protocols supplied by the manufacturer followed by imaging using bright-field microscopy (Olympus BX51TRF, Olympus America, Center Valley, PA).

Determination of tissue myeloperoxidase activity—Tissue myeloperoxidase activity was detected with the FluoroMPO assay purchased from Cell Technology, Inc. (Mountain View, CA). In preparation of this, tissue samples were minced in hexadecyltrimethylammonium bromide buffer (0.5% in 50mM phosphate buffer) on ice and homogenized. The homogenate was sonicated, subjected to a freeze- thaw cycle and centrifuged at 10,000 rpm for 3 minutes. A certain known amount of the tissue lysate supernatant was combined with the detection mix containing H_2O_2, a non-fluorescent detection reagent and 1× assay buffer. The detection reagent is oxidized in the presence of hydrogen peroxide and MPO to produce its fluorescent analog which was measured at an excitation wavelength of 530nm and emission at 590nm. Reported values a normalized to mg of total protein content of the sample.

Statistical Analysis—All data shown are represented as mean ± standard deviation (S.D.). Statistical differences between DSS control and TNF-α NiMOS, TNF-α and scramble sequence-containing NiMOS, and between blank and TNF-α NiMOS groups were determined on both time points using the Student's t-test. P-values less than 0.05 were considered significant; and only significant differences are shown for the sake of clarity.

Results

NiMOS for oral siRNA delivery

An illustration of NiMOS and scanning electron micrographs of siRNA encapsulating gelatin nanoparticles and microspheres is shown in Fig. 1a. Using the solvent displacement method, we were able to produce spherical gelatin nanoparticles encapsulating siRNA with a mean diameter of 279.2±3.2nm. For additional protection from pH and enzymatic degradation during the gastrointestinal transit, the nanoparticles were further encapsulated in PCL microspheres to create NiMOS. These were of fairly uniform shape and size with a relatively smooth surface morphology, and diameters ranging from 2.4 μm to 3.0 μm for siRNA encapsulating and blank microparticles, respectively (Fig. 1b).

To ensure that siRNA was not affected during the manufacturing processes and that particles can efficiently protect this payload in the presence of degrading enzymes, the stability of extracted siRNA was evaluated by agarose gel electrophoresis. As previously shown, NiMOS formulation remain stable under acidic gastric conditions and release the gelatin nanoparticles only in the intestinal pH in the presence of lipase (28). As such, the siRNA stability studies were performed under neutral conditions in the presence of RNAse to show stability of encapsulated duplexes after processing. We found that encapsulation does not affect the structure or size of siRNA (Supplemental Fig. S1). For example, siRNA from gelatin nanoparticles (lane 5) and NiMOS (lanes 7, 8) had the same size as control siRNA (lane 2). Furthermore, protease addition had no adverse effect on siRNA (lane 3).

Additionally, NiMOS appeared to have a protective effect on the payload. This was demonstrated by the band in lane 7; NiMOS were exposed to RNAse A followed by inactivation of the enzyme and extraction of the siRNA revealing a fragment with the same size as control counterparts. However, siRNA released from gelatin nanoparticles was completely degraded when exposed to protease and RNAse, (lanes 6, 9). Exposure of NiMOS to protease alone did not liberate siRNA (no band; lane 11). Quantification of encapsulated siRNA revealed a loading efficiency of 90.2±5.4% in gelatin nanoparticles. Final siRNA loading efficiency in NiMOS was measured to be 55.2±2.8% of the added siRNA.

DSS-induced acute colitis model

After 5 days of DSS administration in drinking water, mice showed typical symptoms of IBD including weight loss, diarrhea, rectal bleeding, and signs of inflammation as evidenced by elevated myeloperoxidase levels, a significant degree of white blood cell infiltration, and abnormal mucosal architecture including goblet cell depletion (Supplementary Fig. S2). The expression profile of TNF-α exhibited highest levels on day 10 of the study before and after which the values were decreased. For this reason, day 10 was chosen as the first time point for evaluation of RNA silencing and its effects on the severity and symptoms of the acute colitis disease model since differences were expected to be at a maximum level at this time point. A second time point was chosen to be seven days after the last oral administration (day 14) to study if the effect of RNA silencing was still persistent.

TNF-α gene silencing

From day 1, female Balb/c mice (6–8 weeks) were induced with acute colitis by addition of 3.5% (w/w) (DSS) in their sole source of drinking water for the duration of the study, while one control group (n=8) received regular tap water during this time. Mice were monitored daily for their health condition including weight loss and stool consistency; after 5–6 days, the disease model was established. Simultaneously, blank or siRNA encapsulating NiMOS (1.2 mg/kg body weight) were orally administered to groups of four animals on day 3, 5, and 7 after an overnight fasting period, as food in the stomach and other sections of the gastrointestinal tract is known to interfere with dosing and analysis upon administration of the formulations. RNA silencing and its effects on the severity and symptoms of the disease model was evaluated at predetermined time points of 10 and 14 days of the study. Four animals per time point and group were sacrificed and their large intestine surgically removed and prepared for subsequent analysis of tissue sections and determination of mRNA and cytokine expression levels. Controls comprised non-treated animals (healthy control group receiving tap water and DSS control administered with DSS water) and NiMOS groups (blank or scramble NiMOS) treated the same as the TNF-α NiMOS group but were instead orally administered with unloaded or inactive/scramble NiMOS. These controls were included in the study to observe potential unspecific or off-target effects.

Quantitative real time PCR (qPCR) analysis was performed to assess expression of murine TNF-α at the mRNA level on day 10 and 14 of the study (Fig. 2a). On day 10, the TNF-α mRNA transcript was lowest in the treatment group receiving TNF-α siRNA encapsulating NiMOS. At this time point, the highest expression levels of the cytokine were observed in the control administered with blank NiMOS which was statistically significant compared to the TNF-α group, while variations between scramble and TNF-α NiMOS groups were not. Slight divergences were observed on day 14 in TNF-α mRNA levels of animals receiving blank, scramble, or TNF-α NiMOS, while the transcript level in the DSS control was highest on both time points and variations in expression patterns between TNF-α and scramble NiMOS administered groups were statistically significant.

Furthermore, murine TNF-α protein levels were determined using a commercially available ELISA (Fig. 2b). Overall, the group receiving TNF-α NiMOS had the lowest expression levels at both time points with an approximate three-fold decrease on day 14. TNF-α levels were higher in blank and inactive NiMOS groups on both days compared to TNF-α NiMOS animals and were of statistical significant differences. However, these levels of protein concentration were lower than in the DSS control group on both time points, which can potentially indicate some off-target effects of NiMOS. Here, we observed an approximate 5-fold increase as compared to levels measured in TNF-α NiMOS treated animals. It is worth mentioning that while blank NiMOS and NiMOS containing control scrambled siRNA sequences appear to have a certain degree of activities themselves, they do not exhibit the same potent gene silencing as well as down-stream biological effects as those shown with TNF-α specific siRNA duplexes in NiMOS. As will be discussed in the following paragraphs, cytokine levels and tissue histological evaluations for the assessment of therapeutic efficacy clearly show that the biological effect is siRNA specific.

Pro-inflammatory cytokine and chemokine profiles

Expression profiles of pro-inflammatory cytokines and chemokines upon oral administration of three doses of NiMOS was measured by ELISA (Fig. 3). Overall, pro-inflammatory cytokines were the lowest in the healthy group (control) that was not exposed to DSS. Therefore, no colitis was induced and no features of inflammation were exhibited. Expression of interleukin (IL)-1β was up-regulated on day 10 in the DSS control group reaching values of 135 pg/mg total protein (Fig. 3b). We observed no substantial decrease in concentration on day 14 in this group. Further, there was no statistically significant difference between NiMOS groups. However, on day 14, concentrations of IL-1β were lowest in the TNF-α NiMOS group in contrast to all other colitis groups showing a 3-, 2-, and 1.5-fold down- regulation compared to the DSS control, blank and inactive NiMOS, respectively. Of all the colitis-bearing animals tested in the study, the lowest concentrations of IL-2, IFN-γ, IL-5, IL-6, and IL-12 p70 (Fig. 3c–f) were measured in the inactive NiMOS group on day 10, indicative of an unspecific reaction in that group, while IL-12p70 levels were the highest in the TNF-α NiMOS group. Statistically significant differences were observed between the TNF-α and scramble NiMOS group in expression profiles of IL-2, IL-5, and IL-6 on both time points and of IFN-γ on day 10. The DSS control had the highest expression levels for the remaining cytokines. As observed in IL-1β, levels of the pro-inflammatory cytokines mentioned above were significantly lower in TNF-α NiMOS animals than in the colitis control group and mock-treatment groups on day 14. On day 10 of the study, levels of granulocyte macrophage colony-stimulating factor (GMCSF) and monocyte inflammatory protein (MIP)-1α did not show any significant variations in all three NiMOS groups; levels were ~1.8 and 13 pg/mg total protein, respectively, while the remaining colitis group reached concentrations of about 2.5 fold of these values (Fig 3g). It should be noted, that the normal concentration of GMCSF was measured to be 0.65 pg/mg total protein, while MIP-1α values were below the detection limit of the assay. Fig. 3h shows that both chemokines were significantly decreased on day 14 in the TNF-α NiMOS group, reaching values of 0.45 pg GMCSF and 4.5 pg MIP-1α per mg total protein for all colitis groups. This is equivalent to a 10-fold and more than a 6-fold decrease of the chemokines as compared to the colitis group and a 6-fold and 3-fold decrease compared to the blank and scramble NiMOS, respectively. Blank and scramble NiMOS exhibited similar levels of these two chemokines, with values of approximately 2.7 pg GMCSF and 13 pg MIP-1α per mg total protein. A similar trend was observed for monocyte chemotactic protein (MCP)-1 for day 14.

Colonic tissue histopathology

H&E stained cryosections from the large intestine were evaluated for changes occurring at the histological level upon induction of acute colitis and treatment of inflammation with TNF-α NiMOS (Fig. 4). Tissue sections from animals within each group exhibited similar histological features. However, for the sake of space, only sections of one animal per group are shown as a representative. Tissue from the control group had normal colon histology bearing no signs of inflammation or disruption of healthy tissue morphology, serving as the baseline for comparison to the remaining samples. In contrast, intestinal tissue from the DSS control, the group receiving blank NiMOS, and scramble NiMOS group exhibited clear signs of inflammation including cell infiltration, goblet cell depletion, and irregular mucosal structure as described before (33), which did not substantially subside as the study progressed. On the other hand, tissue from the TNF-α NiMOS group showed a considerable decrease in the level of inflammation and exhibited a morphological tissue structure resembling that of healthy baseline tissue presenting signs of epithelial regeneration.

Therapeutic efficacy

Changes in body weight of colitis-induced mice were evaluated after administration of various treatments in comparison to the control (Fig. 5). On days 2, 4, and 6, mice from all groups were fasted overnight for consistency, as food in the stomach and other sections of the gastrointestinal tract is known to interfere with dosing and analysis upon administration of the formulations. The following morning they were orally administered with blank, TNF-α or scramble NiMOS. Since fasting caused a weight loss of approximately 10% in all groups (Fig. 5a), mice were administered every other day to allow for normalization of body weight to occur. The weight in the control group stabilized after the last administration leveling out at approximately 5% higher than the weight at the beginning of the study. Weight loss for the DSS control, blank and scramble NiMOS animals was quick after the last oral administration with respective values of 19, 26, and 18% loss of original body weight on day 14. Of all colitis groups, the smallest weight loss of approximately 8% was observed in the TNF-α NiMOS group. Moreover, general appearance was much closer to a healthy mouse in this group with no severe symptoms of colitis as opposed to the remaining colitis mice described before, which exhibited the classical features associated with acute colitis in a considerable number of animals (35). However, there was a slight decrease in body weight after the last oral treatment, which started to increase again on day 11. The faster recovery of body weight in the TNF-α NiMOS compared with the DSS control, blank or scramble NiMOS group was statistically significant ($p=0.015$, $p=0.040$, and 0.049, respectively). Colon length was assessed and is reported in Fig. 5b. Control mice had a colon length of approximately 8.8 cm. A significant reduction in colon length was observed upon induction of DSS colitis with values of approximately 6 cm and is in good agreement with observation reported before (35). Mice treated with blank and scramble sequence siRNA NiMOS also exhibited statistically significant shortening of the colon comparable to the colitis control. For the TNF-α NiMOS group, an increase in colon length to almost 8 cm was observed, which was much closer to the baseline compared to the remaining colitis groups.

Additionally, the activity of myeloperoxidase was measured as an index marker of inflammation based on the infiltration of activated neutrophils (Fig. 5c) (36). Approximately 4 mU and 3 mU/mg total protein were detected in mice upon induction of DSS colitis on day 10 and 14, respectively, which was comparable to the activity observed in the tissue of blank and scramble NiMOS treated animals. MPO activity was lower in the TNF-α NiMOS group at both time points, reaching values of 3.4 and 3.1 mU/mg total protein, respectively. It is worth mentioning, that on day 14, differences in activity between DSS control and TNF-α NiMOS group as well as between TNF-α and scramble NiMOs group were statistically

significant, while this value was not substantially reduced compared to the activity detected in other colitis mice; however it was slighter lower than the baseline value of the healthy control group. This data supports the findings from our histological analysis, where we observed a higher degree of inflammation in DSS control, blank and scramble NiMOS groups, with a slightly lower infiltration on day 14.

Discussion

Due to the limitations associated with the safety and efficacy of conventional IBD treatment, biological therapies are becoming increasingly attractive. With this study, we are attempting to enter into a new era of local IBD treatment that combines positive aspects of RNA interference with the safety of biodegradable polymeric nano- and microparticulate systems enabling a localized treatment through oral administration of siRNA rather than using the traditional systemic approach as reported before (15,20). This option might offer several advantages including lower/fewer doses due to localized therapy and no relative dilution of the agent associated with systemic administration, fewer side effects and higher efficacy. The study conducted by Aouadi *et al.* was one of the first reports of oral siRNA delivery (21). They utilized an encapsulation and delivery system based on β1,3-D-glucan-shells (GeRPs) derived from baker's yeast and observed reduced levels of systemic Map4K4 mRNA in macrophage enriched cells.

We have studied a biodegradable and biocompatible polymeric microsphere based system for oral siRNA delivery. Our previous studies (28) showed that while control gelatin nanoparticles traversed quickly through the gastrointestinal tract upon oral administration, NiMOS had a longer residence time in the small intestine and eventually did accumulate and released their payload in the large intestine. In this study, NiMOS were not targeted to a specific cell population, but expected the released gelatin nanoparticles to be taken up by the enterocytes or immune cells in the colon leading to silencing of upregulated TNF-α in this inflammatory model. Results from our *in vitro* stability study support our hypothesis that NiMOS can effectively protect the siRNA encapsulated within the nanoparticles inside PCL microspheres from the gastrointestinal barriers and degrading proteolytic enzymes; and release is expected to occur in the intestines at the site of inflammation. However, *in vivo* siRNA release studies are difficult to conduct due to rapid degradation of the released nucleic acid constructs and abundant presence of contamination in the GI fluid. As such, we have relied on qPCR and Western blot analysis of gene silencing to support release and intracellular delivery of siRNA from NiMOS. Additionally, the TNF-α gene silencing siRNA sequence for this study was selected from the report by Sorensen *et al.* (15), whose group has performed an extensive analysis with several different anti-TNFα sequences in an *in vitro* assay and selected this particular one as the most potent. While an unmodified siRNA can be potent triggers of the innate immune responses and this could influence the in vivo activity of siRNA owing to off target effects and toxicities associated with immune stimulation, we are convined that any off target effects resulted from this sequence is minimum or none in this case as the TNF-α levels detected (both by mRNA and protein) in the group of mice that had TNF-α siRNA treatment was the least compared to all the other study groups. TNF-α is one of the inflammatory cytokines that is responsive to off target effects and one would expect to see an increase in the levels of this cytokine, if there is an immense off target effect. NiMOS were orally administered to DSS-induced colitis mice followed by evaluation of efficiency and feasibility of RNA silencing involved in inflammation. The disease model was chosen because it is one of the most frequently used rodent IBD models, first discussed by Okayasu et al. in 1990 (35). Supplying DSS in the drinking water of animals *at libitum* provides a predictable onset and course of the disease and lower risk of mortality (33). However, variations of cytokine levels observed in this study are potentially due to the levels of inflammation occurring in the animals (*e.g.*, Fig. 2b

and Fig. S2c). In this acute colitis model, the amount of consumed DSS depends on the volume of water which can be highly variable amongst different animals. Additionally, modulation of DSS-induced colitis by TNF-α reduction remains ambiguous. While some studies suggest that TNF-α may play a protective role in the initial phase of DSS colitis (37) other studies involving siRNA mediated gene silencing have reported decreased severity of inflammation after downregulation of this protein (20,38).

In the TNF-α NiMOS group, the analysis of real time PCR of both time points showed very low levels of murine TNF-α, which was similar to the level observed in healthy, control mice on day 10. This can be attributed to the silencing effect of NiMOS, which was not observed in remaining colitis-bearing groups. Increased TNF-α mRNA in NiMOS control groups (blank and scramble) were comparable to levels observed in the DSS control and can potentially be ascribed to an unspecific immune response elicited by NiMOS and/or inactive siRNA sequence itself. The siRNA sequence used in this study was not modified, so that an elicitation of the immune system becomes possible. Although this is the case, any off target effects that could be resulting from this sequence is believed to be minimum or none in this study as the TNF-α levels detected (both by mRNA and protein) in the group of mice that had TNF-α siRNA treatment was the least compared to all the other study groups. Given the fact that TNF-α is one of the inflammatory cytokines that is responsive to off target effects, one would expect to see an increase if there is an immense off target effect. However, future studies will be performed including modified and non-immune stimulatory siRNA as control to address this issue. Also, different target-specific siRNA sequences capable of silencing TNF-α will also be incorporated to study potential off-target effects arising from the encapsulation system or the siRNA itself.

On day 14, a relative decrease in expression of TNF-α mRNA was observed in all NiMOS groups which can potentially be attributed to a complex interplay of pro-and anti-inflammatory cytokines resulting in compensatory responses due to induction of colitis. ELISA results were in good correlation with real time-PCR analysis. Lower levels of TNF-α were observed in TNF-α NiMOS animals as compared to the remaining colitis-bearing groups at both time points and most cytokines on day 14 indicating the high potential of TNF-α siRNA NiMOS for oral administration and RNA silencing, while elevated levels of pro-inflammatory cytokines where detected in blank and scramble NiMOS groups. Based on our initial hypothesis, lower expression of many cytokines due to down-regulation of TNF-α could likely result in alleviation of inflammation at the disease site. This was also reflected in the smaller degree of weight loss and in colon tissue morphology which showed signs of regeneration with only few abnormalities. On the other hand, tissue from other groups showed clear signs of inflammation including cell infiltration, ulcers and destruction of regular mucosal architecture. Shortly after the last administration of all three NiMOS doses, downregulation of the cytokines was not as pronounced in the TNF-α group, and expression levels were slightly higher compared to remaining NiMOS controls. This effect could be attributed to the specificity of the TNF-α siRNA, which resulted in silencing of TNF-α and had no immediate effect on other markers after a short time. Also, lower expression of TNF-α due to silencing in this group preceded the downregulation of other pro- inflammatory cytokines. Moreover, we saw a reduction of expression on day 14 in certain chemokines such as GMCSF, MIP-1α, and MCP-1, which are markers regulating cell infiltration at disease sites, thus directly contributing to inflammatory responses. For example, systemic administration of MIP-1α has been shown to considerably aggravate colitis in mouse models (39). Thus, lower expression levels of MIP-1α as observed in TNF-α NiMOS groups indicates alleviation of the disease suggesting the therapeutic efficacy of TNF-α silencing treatment. However, inactive and blank NiMOS had some effect on downregulation of IL-1β, IL-5, MIP-1α, and GMCSF compared to the DSS control on day 10. As mentioned before, NiMOS itself as well as un-modified siRNA sequence used might have an immune-

modulatory effect and can affect some of the results; thus, it is an important control in this study.

While this system needs further improvement and optimization, results show the potential of NiMOS as a therapeutic option for treatment of IBD. Furthermore, silencing of TNF-α might not be sufficient to diminish the severity of the disease in this scenario, so that future projects will involve orally administered formulations encapsulating a combination of therapeutic siRNA to silence proteins of interest locally at the disease site and allow for the treatment of inflammatory bowel disease.

Supplementary Material

Refer to Web version on PubMed Central for supplementary material.

Acknowledgments

This study was supported by a grant (R01-DK080477) from the National Institute of Diabetes, Digestive Diseases, and Kidney Diseases of the National Institutes of Health. Ms. Shanthi Ganesh's assistance with the critical review of the manuscript and suggestions is also deeply appreciated. We are also grateful to Dr. David Nguyen in Professor Robert Langer's lab at MIT (Cambridge, MA) for the use of the Coulter particle size analysis instrument and to Mr. William Fowle who assisted with scanning electron microscopy at the Nano-Instrumentation Facility at Northeastern University (Boston, MA).

References

1. Bouma G, Strober W. The immunological and genetic basis of inflammatory bowel disease. Nature Reviews Immunology 2003;3:521–533.
2. Strober W, Fuss I, Mannon P. The fundamental basis of inflammatory bowel disease. Journal of Clinical Investigation 2007;117:514–521. [PubMed: 17332878]
3. Ardizzone S, Porro GB. Biologic therapy for inflammatory bowel disease. Drugs 2005;65:2253–2286. [PubMed: 16266194]
4. Oldenburg B, Hommes D. Biological therapies in inflammatory bowel disease: top-down or bottom-up? Current Opinion in Gastroenterology 2007;23:395–399. [PubMed: 17545775]
5. Sandborn WJ. Strategies for targeting tumour necrosis factor in IBD. Best Practice & Research in Clinical Gastroenterology 2003;17:105–117.
6. Stokkers PCF, Hommes DW. Novel biological therapies for inflammatory bowel disease. Curr Treat Options Gastroenterol 2006;9:201–210. [PubMed: 16901384]
7. Mueller C. Tumour necrosis factor in mouse models of chronic intestinal inflammation. Immunology 2002;105:1–8. [PubMed: 11849309]
8. van Deventer SJH. New biological therapies in inflammatory bowel disease. Best Practice & Research in Clinical Gastroenterology 2003;17:119–130.
9. Papa A, Mocci G, Bonizzi M, Felice C, Andrisani G, Papa G, Gasbarrini A. Biological therapies for inflammatory bowel disease: controversies and future options. Expert Review of Clinical Pharmacology 2009;2:391–403.
10. Hoentjen F, Van Bodegraven AA. Safety of anti-tumor necrosis factor therapy in inflammatory bowel disease. World Journal of Gastroenterology 2009;15:2067–2073. [PubMed: 19418577]
11. Mannon PJ, Fuss IJ, Mayer L, Elson CO, Sandborn WJ, Present D, Dolin B, Goodman N, Groden C, Hornung RL, Quezado M, Neurath MF, Salfeld J, Veldman GM, Schwertschlag U, Strober W. Anti–Interleukin-12 Antibody for Active Crohn's Disease. The New England Journal of Medicine 2004;351:2069–2079. [PubMed: 15537905]
12. Ito H, Takazoe M, Fukuda Y, Hibi T, Kusugami K, Andoh A, Matsumoto T, Yamamura T, Azuma J, Nishimoto N, Yoshizaki K, Shimoyama T, Kishimoto T. A pilot randomized trial of a human anti–Interleukin-6 receptor monoclonal antibody in active Crohn's disease. Gastroenterology 2004;126:989–996. [PubMed: 15057738]

13. Sandborn WJ, Colombel JF, Enns R, Feagan BG, Hanauer SB, Lawrance IC, Panaccione R, Sanders M, Schreiber S, Targan S, van Deventer S, Goldblum R, Despain D, Hogge GS, Rutgeerts P. Natalizumab induction and maintenance therapy for Crohn's disease. New England Journal of Medicine 2005;353:1912–1925. [PubMed: 16267322]

14. Feagan BG, Greenberg GR, Wild G, Fedorak RN, Paré P, McDonald JW, Dubé R, Cohen A, Steinhart AH, Landau S, Aguzzi RA, Fox IH, Vandervoort MK. Treatment of ulcerative colitis with a humanized antibody to the alpha4beta7 integrin. New England Journal of Medicine 2005;352:2499–2507. [PubMed: 15958805]

15. Sorensen DR, Leirdal M, Sioud M. Gene silencing by systemic delivery of synthetic siRNAs in adult mice. Journal of Molecular Biology 2003;327:761–766. [PubMed: 12654261]

16. Armuzzi A, De Pascalis B, Lupascu A, Fedeli P, Leo D, Mentella MC, Vincenti F, Melina D, Gasbarrini G, Pola P, Gasbarrini A. Infliximab in the treatment of steroid-dependent ulcerative colitis. European Review for Medical Pharmacological Sciences 2004;8:231–233.

17. MacDiarmid JA, Amaro-Mugridge NB, Madrid-Weiss J, Sedliarou I, Wetzel S, Kochar K, Brahmbhatt VN, Phillips L, Pattison ST, Petti C, Stillman B, Graham RM, Brahmbhatt H. Sequential treatment of drug-resistant tumors with targeted minicells containing siRNA or a cytotoxic drug. Nature Biotechnology 2009;27:643–U697.

18. Kortylewski M, Swiderski P, Herrmann A, Wang L, Kowolik C, Kujawski M, Lee H, Scuto A, Liu Y, Yang C, Deng J, Soifer HS, Raubitschek A, Forman S, Rossi JJ, Pardoll DM, Jove R, Yu H. In vivo delivery of siRNA to immune cells by conjugation to a TLR9 agonist enhances antitumor immune responses. Nature Biotechnology 2009;27:925–932.

19. Choi B, Hwang Y, Kwon HJ, Lee ES, Park KS, Bang D, Lee S, Sohn S. Tumor necrosis factor alpha small interfering RNA decreases herpes simplex virus-induced inflammation in a mouse model. Journal of Dermatological Science 2008;52:87–97. [PubMed: 18585901]

20. Peer D, Park EJ, Morishita Y, Carman CV, Shimaoka M. Systemic leukocyte-directed siRNA delivery revealing cyclin D1 as an anti-inflammatory target. Science 2008;319:627–630. [PubMed: 18239128]

21. Aouadi M, Tesz GJ, Nicoloro SM, Wang MX, Chouinard M, Soto E, Ostroff GR, Czech MP. Orally delivered siRNA targeting macrophage Map4k4 suppresses systemic inflammation. Nature 2009;458:1180–U1116. [PubMed: 19407801]

22. Sioud M. On the delivery of small interfering RNAs into mammalian cells. Expert Opinion on Drug Delivery 2005;2:639–651. [PubMed: 16296791]

23. Xu D, McCarty D, Fernandes A, Fisher M, Samulski RJ, Juliano RL. Delivery of MDR1 small interfering RNA by self-complementary recombinant adeno-associated virus vector. Molecular Therapy 2005;11:523–530. [PubMed: 15771955]

24. Fattal E, Bochot A. State of the art and perspectives for the delivery of antisense oligonucleotides and siRNA by polymeric nanocarriers. International Journal of Pharmaceutics 2008;364:237–248. [PubMed: 18619528]

25. Bhavsar MD, Amiji MM. Development of novel biodegradable polymeric nanoparticles-in-microsphere formulation for local plasmid DNA delivery in the gastrointestinal tract. AAPS PharmScitech 2008;9:288–294. [PubMed: 18446494]

26. Bhavsar MD, Amiji MM. Polymeric nano- and microparticle technologies for oral gene delivery. Expert Opinion on Drug Delivery 2007;4:197–213. [PubMed: 17489649]

27. Bhavsar MD, Amiji MM. Oral IL-10 gene delivery in a microsphere-based formulation for local transfection and therapeutic efficacy in inflammatory bowel disease. Gene Therapy 2008;15:1200–1209. [PubMed: 18418416]

28. Bhavsar MD, Amiji MM. Gastrointestinal distribution and in vivo gene transfection studies with nanoparticles-in-microsphere oral system (NiMOS). Journal of Controlled Release 2007;119:339–348. [PubMed: 17475358]

29. Kaul G, Amiji M. Tumor-targeted gene delivery using poly(ethylene glycol)-modified gelatin nanoparticles: In vitro and in vivo studies. Pharmaceutical Research 2005;22:951–961. [PubMed: 15948039]

30. Bhavsar MD, Tiwari SB, Amiji MM. Formulation optimization for the nanoparticles-in-microsphere hybrid oral delivery system using factorial design. Journal of Controlled Release 2006;110:422–430. [PubMed: 16338017]

31. Diez S, de Ilarduya CT. Versatility of biodegradable poly(D,L-lactic-co-glycolic acid) microspheres for plasmid DNA delivery. European Journal of Pharmaceutics and Biopharmaceutics 2006;63:188–197. [PubMed: 16697172]

32. Tracy M. Development and scale-up of a microsphere protein delivery system. Biotechnological Progress 1998;14:108–115.

33. Melgar S, Karlsson A, Michaelsson EM. Acute colitis induced by dextran sulfate sodium progresses to chronicity in C57BL/6 but not in BALB/c mice: correlation between symptoms and inflammation. American Journal of Physiology-Gastrointestinal and Liver Physiology 2005;288:G1328–G1338. [PubMed: 15637179]

34. Barbara G, Xing Z, Hogaboam CM, Gauldie J, Collins SM. Interleukin 10 gene transfer prevents experimental colitis in rats. Gut 2000;46:344–349. [PubMed: 10673295]

35. Okayasu I, Hatakeyama S, Yamada M, Ohkusa T, Inagaki Y, Nakaya R. A novel method in the induction of reliable experimental acute and chronic ulcerative-colitis in mice. Gastroenterology 1990;98:694–702. [PubMed: 1688816]

36. Grisham MB, Benoit JN, Granger DN. Assessment of leukocyte involvement during ischemia and reperfusion of intestine. Methods in Enzymology 1990;186:729–742. [PubMed: 2172726]

37. Kojouharoff G, Hans W, Obermeier F, Mannel DN, Andus T, Scholmerich J, Gross V, Falk W. Neutralization of tumour necrosis factor (TNF) but not of IL-1 reduces inflammation in chronic dextran sulphate sodium-induced colitis in mice. Clinical and Experimental Immunology 1997;107:353–358. [PubMed: 9030875]

38. Zhang YJ, Cristofaro P, Silbermann R, Pusch O, Boden D, Konkin T, Hovanesian V, Monfils PR, Resnick M, Moss SF, Ramratnam B. Engineering mucosal RNA interference in vivo. Molecular Therapy 2006;14:336–342. [PubMed: 16766229]

39. Pender SLF, Chance V, Whiting CV, Buckley M, Edwards M, Pettipher R, MacDonald TT. Systemic administration of the chemokine macrophage inflammatory protein 1a exacerbates inflammatory bowel disease in a mouse model. Gut 2005;54:1114–1120. [PubMed: 16009684]

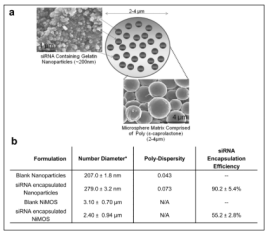

Figure 1.

(a) Schematic representation of the NiMOS and the scanning electron micrographs of small interfering RNA (siRNA)-encapsulated type B gelatin nanoparticles and siRNA-containing NiMOS and (b) the particle size and siRNA encapsulation efficiency in gelatin nanoparticles and NiMOS.

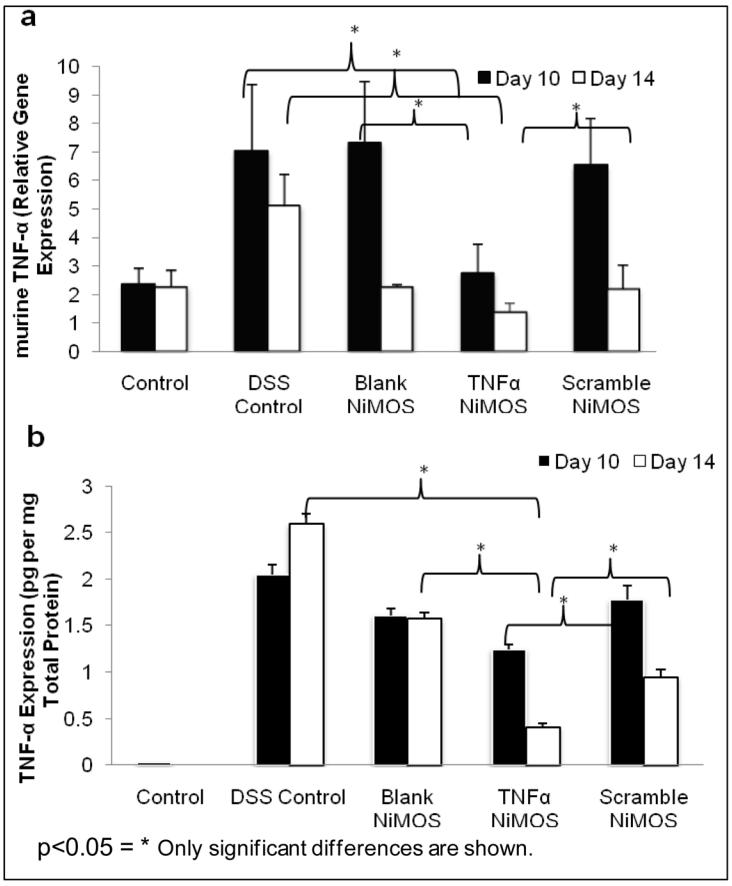

Figure 2.

Murine TNF-α expression upon oral delivery of siRNA against TNF-α using NiMOS in a dextran sulfate (DSS)-induced acute colitis mouse model. a) Quantitative real time-PCR analysis performed on samples of the large intestines obtained from control and experimental treatment groups showing lower mRNA transcript upon oral administration of siRNA with NiMOS. b) Levels of TNF-α as determined by ELISA.

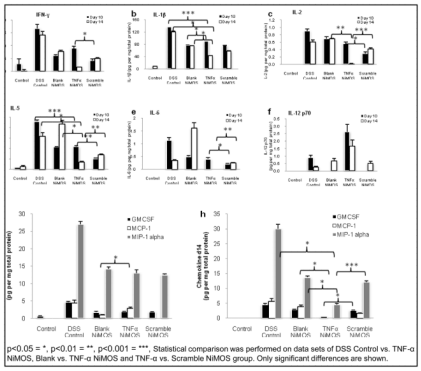

Figure 3.

Cytokine and chemokine profiles in the GI tract of control and TNF- a silencing siRNA administration using NiMOS. Concentrations of a) Interferon gamma (IFN)-γ), b) Interleukin (IL)-1β, c) IL-2, d) IL-5, e) IL-6, and f) IL-12 p70 as well as (g,h) chemokines in the large intestine are shown.

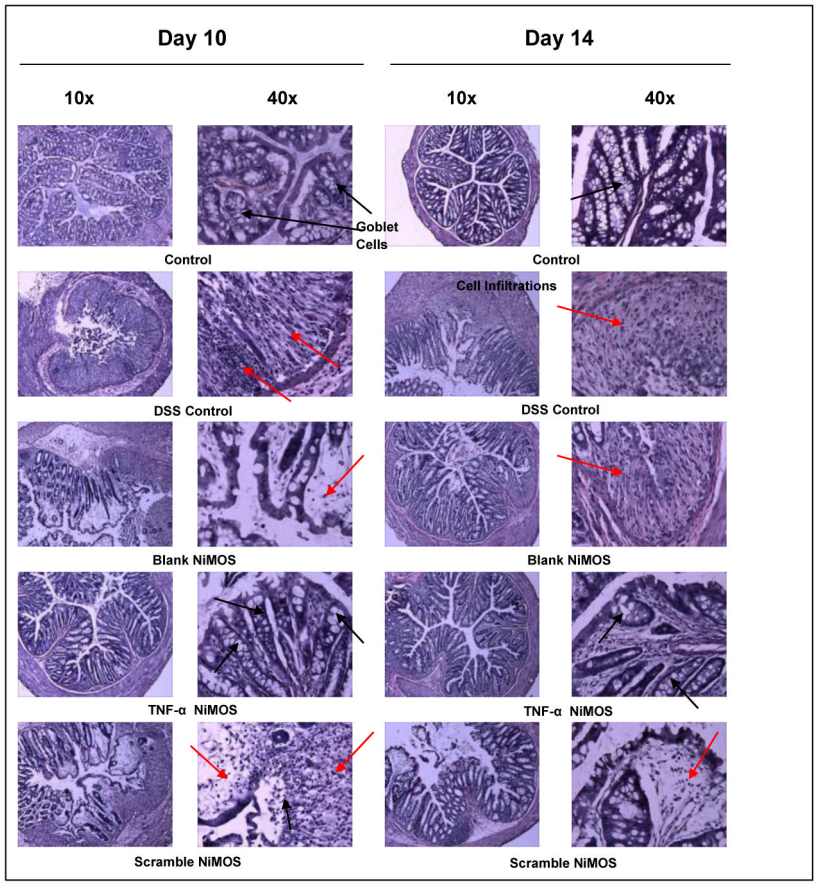

Figure 4.

H&E stained sections of the colon harvested from each group at days post-administration. Images of tissue cryosections obtained on day 10 and day 14 of the study are shown at magnifications of 10× and 40× of the original size. Occurrence of goblet cells is indicated by red arrows; cell infiltration and abnormal tissue histology is indicated by black arrows.

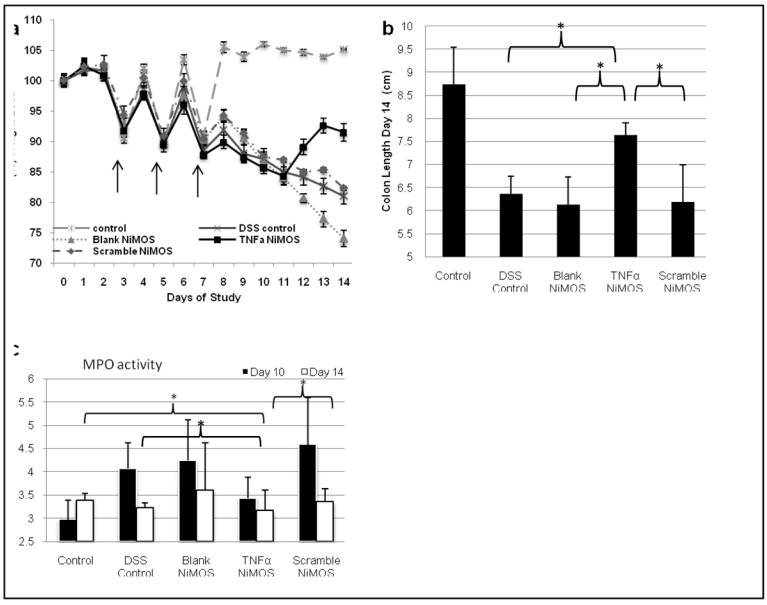

Figure 5.

(a) Percent change in body weight of Balb/c mice upon continuous exposure to DSS for development of acute colitis model. (b) Measurement of colon length on day 14. (c) Tissue myeloperoxidase activity in the large intestine normalized to the total protein content of each sample. $p < 0.05$ = *, Only significant differences are shown.